Self-replicating colloidal clusters

Zorana Zeravcic[a,b,1] and Michael P. Brenner[a,b]

[a]School of Engineering and Applied Sciences and [b]Kavli Institute for Bionano Science and Technology, Harvard University, Cambridge, MA 02138

We construct schemes for self-replicating clusters of spherical particles, validated with computer simulations in a finite-temperature heat bath. Each particle has stickers uniformly distributed over its surface, and the rules for self-replication are encoded into the specificity and strength of interactions. Geometrical constraints imply that a compact cluster can copy itself only with help of a catalyst, a smaller cluster that increases the surface area to form a template. Replication efficiency requires optimizing interaction energies to destabilize all kinetic traps along the reaction pathway, as well as initiating a trigger event that specifies when the new cluster disassociates from its parent. Although there is a reasonably wide parameter range for self-replication, there is a subtle balance between the speed of the reaction, and the error rate. As a proof of principle, we construct interactions that self-replicate an octahedron, requiring a two-particle dimer for a catalyst. The resulting self-replication scheme is a hypercycle, and computer simulations confirm the exponential growth of both octahedron and catalyst replicas.

self-assembly | catalytic cycle

The ability to invent materials that replicate themselves could lead to a paradigm shift in materials discovery. The exponential amplification of biological molecules, followed by mutation and selection, has allowed the development of powerful protocols for evolving proteins with improved catalytic properties (1, 2). However, whereas modern materials science excels at synthesis, there has been much less success at building artificial self-replicating materials. If there were methods for self-replicating complex materials, then selection–amplification cycles would surely discover solutions with greatly enhanced properties.

The logical framework required for objects to replicate themselves was given by von Neumann. He gave an explicit construction of a self-replicating 2D lattice of coupled cellular automata (3), in which a finite area of the lattice replicates itself on an adjacent region. Over the years, von Neumann's schemes have been refined (4–8), but an efficiently self-replicating artificial system has never been physically realized. To date, artificial self-replicating systems have focused on linear chain-like structures, where the replicate is templated on the original, closely analogous to DNA, whose replication machinery was unknown at the time of von Neumann's writings. For example, Seeman and coworkers (9) have recently described and experimentally demonstrated the creation of a self-replicating DNA-based material, using tile motifs with specific binding at their edges and faces. In their scheme, the replication of each generation is achieved by manipulating chemistry and temperature, with complementary motifs manually separated from the initial sequence. The newly formed generation is an accurate copy about one-third of time. Although this is a step in the desired direction, this setup does not achieve exponential growth, and moreover this type of protocol is restricted to linear chain-like molecules.

In this paper, we present explicit examples of physical interactions between spheres in a finite-temperature bath that lead to self-replication of clusters, in a manner that is geometrically distinct from replicating reactions of linear chains. Although our examples were inspired by recent experiments with colloidal spheres or nanoparticles coated with DNA, we believe that our construction is sufficiently general that it might prove implementable with a broader class of materials, such as protein complexes

with designed interactions (10). We make no attempt to construct a self-replicating material of minimal complexity, but instead endeavor to show that efficient schemes exist, where the errors caused by thermal fluctuations into misfolded states do not inhibit the replication reaction.

In our examples, each sphere has stickers distributed uniformly over its surface, causing short-ranged, specific interactions with other spheres. The rules for self-replication are encoded into the specificity and strength of the interactions. Bond strengths must be chosen not only to respect the geometry of the desired self-replication reaction, but also, critically, to avoid kinetic traps. We find that self-replicating a compact cluster requires a specifically designed catalyst, a smaller cluster that allows the parent to template itself from a finite-concentration monomer bath. Additionally, efficient self-replication requires specifying an allosteric trigger event, where the daughter structure separates from the parent, and the bonds within the daughter stabilize. The self-replication reactions we outline replicate both the parent cluster and the catalyst, so that a single catalyst and cluster are sufficient for exponential growth of both. Computer simulations of interacting particles in a thermal bath verify that the design interactions lead to efficient self-replication.

For definiteness, we focus on a detailed scheme for the specific case of a self-replicating octahedron, as shown in Fig. 1A. The first step is the design of the initial seed octahedron (red particles). Octahedron is one of the two rigid (ground-state) structures, having 12 contacts, that can be formed out of 6 colloidal particles, the other being a polytetrahedron. When self-assembling from identical particles, the yield of octahedra is ∼4% and that of the polytetrahedra is ∼96%, the difference stemming from rotational entropy (11, 12). If, however, particles are not identical but have stickers that are chosen to satisfy certain interaction rules (13), octahedron becomes the only ground-state structure that can be self-assembled, and therefore the yield is improved

Significance

One of the hallmarks of living systems is self-replication. Mimicking nature's ability to self-replicate would not only give more insight into biological mechanisms of self-replication but also could potentially revolutionize material science and nanotechnology. Over the past 60 y, much research, both theoretical and experimental, has been focused on understanding and realizing self-replicating systems. However, artificial systems that efficiently self-replicate remained elusive. In this paper, we construct schemes for self-replication of small clusters of isotropic particles. By manipulating the energy landscape of the process, we show how exponential replication can be achieved. As a proof of principle, we show exponential self-replication of an octahedral cluster using finite-temperature computer simulations.
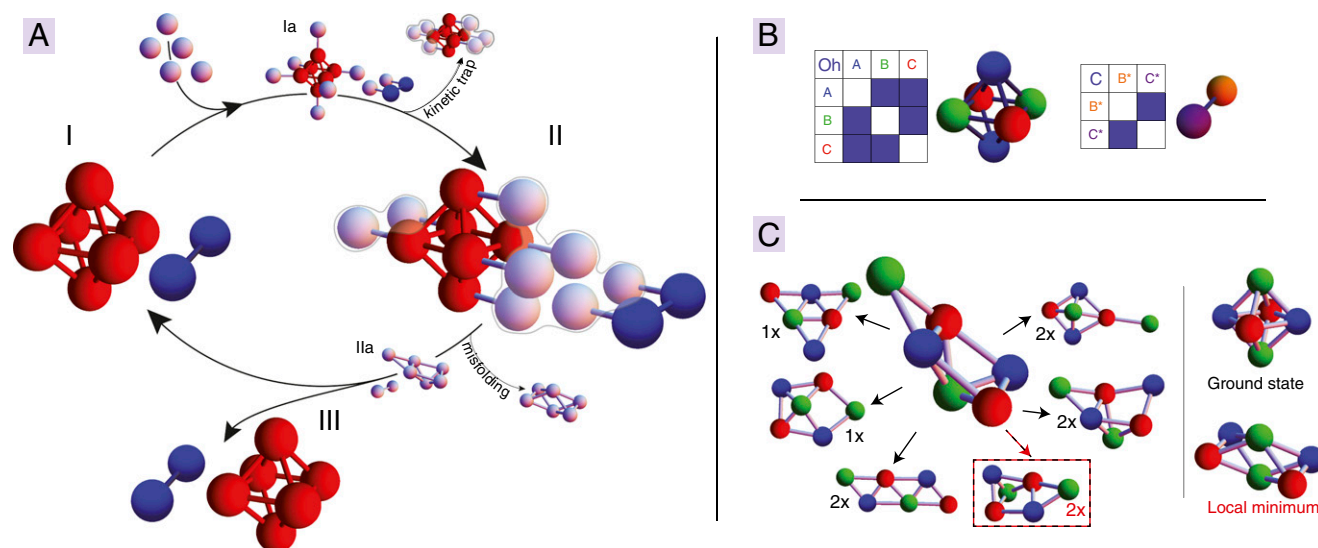
Fig. 1. Self-replication scheme for an octahedron. (*A*) Self-sustained reaction scheme for self-replication of an octahedron Oh (red particles). A minimal catalyst needed for the replication is a dimer (blue particles). Only one appropriately labeled monomer (gray particles) per particle in Oh/catalyst can be attached (stage Ia). Attached monomers can now interact between themselves and form substructures templated by the Oh and the catalyst (stage II). Once a certain number of bonds between these monomers forms, melting occurs, separating starting Oh and catalyst from attached monomers (stage IIa). New structures formed produce a new catalyst and a nonrigid cluster that folds into a new octahedron (stage III). Along this cycle, there are two undesirable branches: (*i*) after stage Ia, the Oh–monomer complex can end up in a kinetic trap, and (*ii*) after the melting occurs (stage II), the new structure can misfold into a local minimum. (*B*) Interaction matrices for the octahedron and the catalyst. Bonds within these clusters are irreversible. (*C*) All 9-contact floppy transient structures made by removing one bond from the 10-contact floppy transient structure. Numbers next to these structures indicate their stoichiometric factors. Nine out of 10 structures fold into an octahedron. The one framed can also fold into the lowest-energy local minimum.

(see *SI Text* and Figs. S1 and S2 for more details). This choice of interaction rules (Fig. 1*B*) has three types of particles, labeled blue (*A*), green (*B*), and red (*C*), where like particles do not stick to each other, but do stick to the other particle types.

Generally, a scheme for self-replication requires the seed octahedron to act as a template for the formation of another octahedron. Each particle in the seed can bind to another (complementary) particle from the solution of monomers. Attached particles can interact between themselves, resulting in templated substructures. However, these interactions alone are still insufficient for producing an octahedron, because the geometrical backbone of the seed is too rigid for the attached particles to flex into an octahedral shape. This can instead be achieved with the presence of a catalyst, and we find that it is sufficient for the catalyst to consist of a dimer (blue particles in Fig. 1*A*). The dimer has two particle types labeled purple (C^*) and orange (B^*), with the interaction matrix shown in Fig. 1*B*.

As shown in Fig. 1*A*, the catalyst can bind two (appropriate) monomers from the solution (stage Ia) and together with four particles bound to the seed octahedron form a six-particle monomer structure (stage II), which gives rise to the octahedron replica when "melting" is triggered (stage IIa and III). This cycle is self-sustained because the remaining two monomers bound to the seed octahedron become a catalyst dimer after melting (stage IIa and III). The melting process refers to breaking of the single bond that connects a monomer to the seed octahedron or the catalyst, and is triggered for all monomers in stage II when the total number of bonds between them reaches a predetermined value n_c. Once melting occurs, we assume that the bonds formed between the monomers become irreversible.

Setting the value of n_c is crucial because it strongly influences the balance between replication efficiency and error rate. By the very nature of templating from a 3D cluster, the melting produces a floppy transient structure of monomers (having n_c bonds), which ideally should fold into a geometrical copy of the octahedron (see stage IIa in Fig. 1*A*). In our construction

(Fig. 1*A*), the maximum geometrically possible value of n_c^{max} is 10. For $n_c = 10$, the transient structure can only fold into the octahedron. For $n_c = 9$, Fig. 1*C* shows that 9 out of 10 possible outcomes of folding is the octahedron. Although this gives a rough estimate of the error rate to be 10%, our simulations indicate it is smaller, implying that entropic factors are significant. In general, with decreasing n_c, the melting happens more frequently but with a higher error rate. An optimal value of n_c depends on the energy landscape of the cluster in question, and we will discuss this in more detail below.

The geometric scheme for self-replication analyzed so far (Fig. 1*A*) can be turned into a precise reaction scheme (Fig. 2*A*) with 10 different particle types. The particles A, B, and C in the seed octahedron can bind to their complementary particle type A', B', and C' from the solution of monomers if the particles were coated with DNA, a monomer attaching to a seed particle would have the appropriate complementary strand. Similarly, the catalyst particles C^* and B^* bind to complementary monomers $C^{*'}$ and $B^{*'}$ from the solution. The complete interaction matrix for all particle types is shown in Fig. 2*B*.

The interaction rules imply that an A, B, C-type octahedron seed with a C^*, B^*-type dimer creates a new octahedron made of particle types A', B', C' and a new dimer of type $C^{*'}, B^{*'}$. The newly created octahedron and dimer can now bind monomers and take part in a melting process that will create their complements, i.e., an A, B, C-type octahedron and a C^*, B^*-type dimer, closing the two-step replication cycle. As Fig. 2*A* illustrates, the entire self-replication process of two complementary types of octahedra is a hypercycle (14–17), consisting of two linked catalytic cycles.

We test the reaction scheme using dissipative particle dynamics (DPD) techniques (18, 19). Our simulation contains colloidal spheres of diameter D, with an interaction range of $1.05D$. The colloids are immersed into a DPD solvent of smaller particles. We simulated systems with 96, 256, and 512 colloidal particles, out of which 6 comprise the parent octahedron and 2 the catalyst. Simulations are run at a fixed temperature with
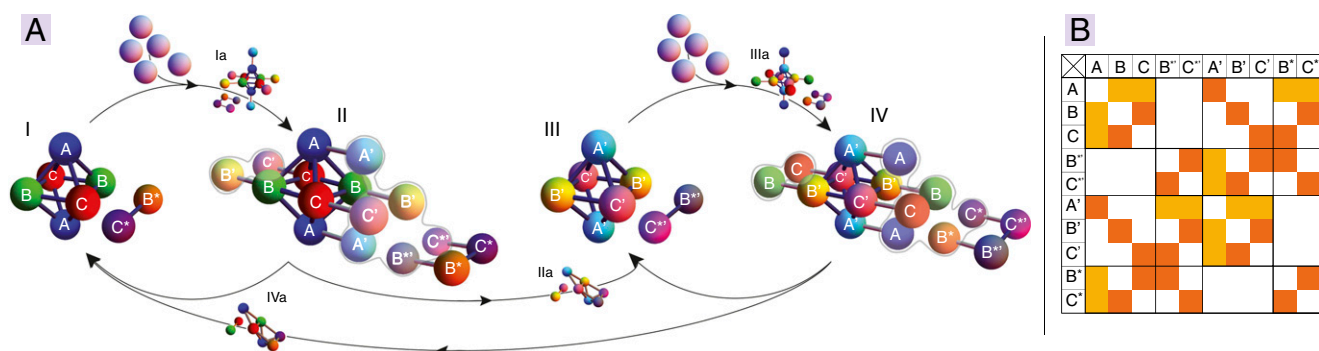
Fig. 2. A detailed self-replication scheme for an octahedron. (*A*) The reaction scheme. (*B*) Full interaction matrix between particle types present in the simulation. Interactions between particle types A/A' and $B,C,B^*,C^*/B',C',B^*,C^*$ (colored light orange) are weaker than the other interactions (dark orange). The ratio of these bond strengths is optimized (*SI Text*). Once particles form an octahedron or a catalyst, their bonds become irreversible.

a volume fraction of colloids $\phi_{coll} = 0.01$, and a larger volume fraction of solvent $\phi_{sol} \approx 0.2$. More details are given in *SI Text*.

Even with a geometrically compatible scheme for self-replication, a successful implementation still requires an extensive search for both bond strengths and the characteristics of the disassociation reaction n_c. With bond optimization, and the value

$n_c = 9$, Fig. 3 presents typical snapshots of a simulation showing successful self-replication, where different phases of the reaction cycle can be recognized. Fig. 3*A* shows exponential growth of the number of octahedra, as expected for a hypercycle.

Such robust results rely critically on avoiding traps along the self-replication reaction pathway, requiring careful choice of
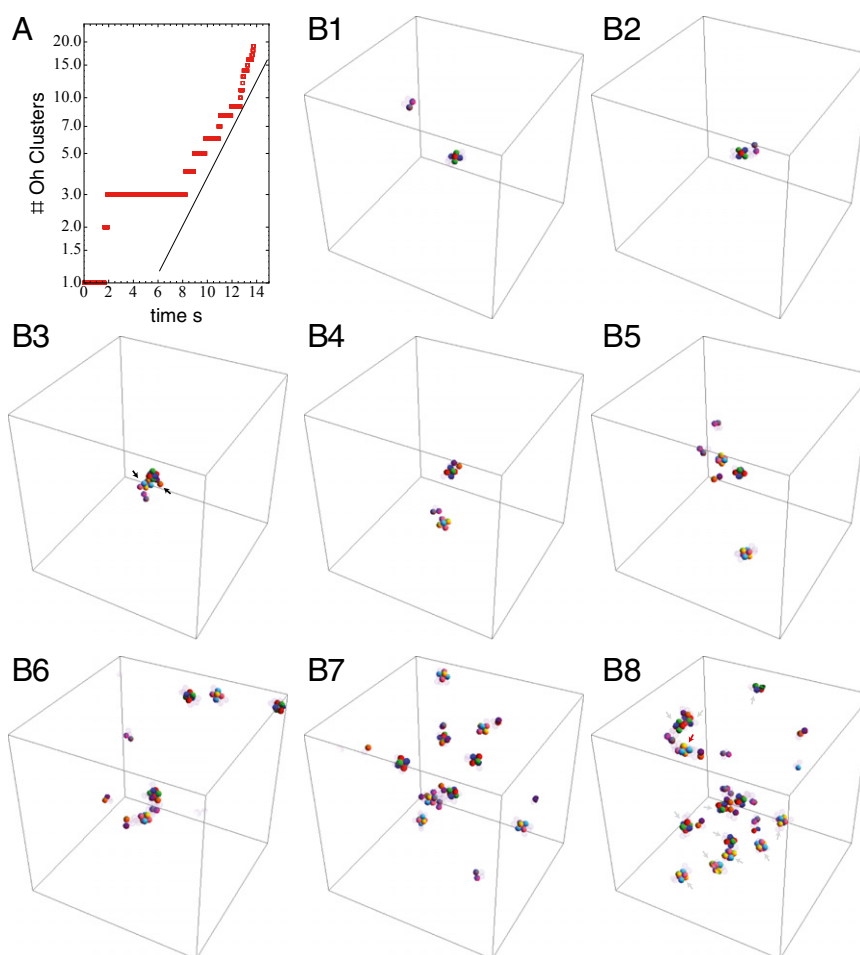

Fig. 3. DPD simulation of octahedron self-replication using 512 colloidal particles. (*A*) The total number of octahedra (both *ABC* and *A'B'C'*) as function of time. The black line $\sim e^x$ is a guide for the eye. (*B1*–*B8*) Typical snapshots of a simulation (see *SI Text* for the movie). Colloids are colored if they comprise an Oh or a catalyst (color scheme like in Fig. 2*A*). Monomers are in general not shown unless they are attached to an Oh/catalyst (transparent spheres). These snapshots reveal phases of the reaction cycle (Fig. 2*A*). For example, *B3* shows a melting process, after which in *B4* a new octahedron is formed together with a new catalyst. In *B8*, there are 12 octahedral clusters apart from the initial seed. One of the replicas (marked with a red arrow) is a misfolded octahedron.

both bond strengths and the melting criterion. The first kinetic trap that can impede the self-replication of the octahedron occurs during the initial attachment of the monomers (after stage Ia in Fig. 1*A*); the attached monomers can form two triangles attached on opposite faces of the octahedron. This configuration is relatively frequent and stable due to the octahedral symmetry. The bond optimization must break this symmetry of bonds within a triangle, disfavoring this configuration. Kinetic traps in a later stage of the hypercycle (after stage II in Fig. 1*A*) can also occur due to the choice of n_c. The maximum value of n_c is determined by the geometry of the template. For the octahedron with a dimer enzyme, $n_c^{max} = 10$. There is also a minimum value of $n_c = n_c^{gs}$, where the floppy transient structure obtained by melting can fold only into the desired cluster. The value of n_c^{gs} depends on the geometry of the lowest energy local minima where kinetic traps can occur. For the octahedron, the lowest energy local minimum (Fig. 1*C*) has two bonds less (10) than the ground state (12), and three bonds need to be broken to transform the ground state into that local minimum. This implies $n_c^{gs} = (12 - 3) + 1 = 10$.

The mentioned lowest-energy local minimum can actually still act as a template for replicating an octahedron, albeit with a smaller replication rate because, e.g., the red–green–red–green face and blue–green–blue–green face (Fig. 1*C*) cannot template a replica. The property that the local minimum can only template a copy of an octahedron is exceptional, and holds because the octahedron is a small and highly symmetric cluster.

How large is the parameter range available for self-replication? One way to assess this is to consider a situation where there is a fixed concentration of the different monomers, and the catalyst dimer, and write the kinetic differential equations that govern transitions between different states of the hypercycle as labeled in Fig. 1*A* (see *SI Text* for explicit equations). Several of the parameters (e.g., the attachment of monomers onto the parent octahedron) are set by diffusion, so as a choice of normalization we set these equal to unity. Three key parameters can be tuned with the bond strengths and n_c: (*i*) the rate $k_{kinetic\ trap}$, at which the stage I octahedron transitions to the initial kinetic trap; (*ii*) the rate $k_{melting}$, at which the melting criterion is satisfied from the stage II octahedron–catalyst complex; and (*iii*) the rate $k_{misfolding}$, at which the melted structure misfolds into something other than an octahedron. Keeping in mind that there is a lower bound on the bond strengths set by the temperature of the experiment, we can choose bond strengths so that the initial kinetic trap is effectively suppressed. By solving the differential equations (*SI Text*) and extracting the exponential growth rate of octahedra, we arrive at the replication phase diagram in Fig. 4, which shows that exponential self-replication occurs whenever misfolding is sufficiently low, independently of the value of melting rate constant.

Generally, with a more stringent melting criterion (i.e., larger n_c), $k_{misfolding}$ decreases because there are less pathways available for the floppy structure to misfold. Quantitatively, the misfolding rate is roughly the ratio of numbers of ways the floppy structure can fold into a local minimum versus into the desired cluster. Fig. 1*C* shows that, for the octahedron, if $n_c = 10$, $k_{misfolding} = 0$, if $n_c = 9$, $k_{misfolding} \sim 1/10$, if $n_c = 8$, $k_{misfolding} \sim 1/6$, and so on, where the rates are measured in the units of a typical rate constant set by diffusion. This means that small $k_{misfolding}$ (i.e., exponential replication) can be generically achieved by simply choosing a sufficiently large n_c. The rate $k_{melting}$ likewise decreases with increasing n_c, and hence is not independent of $k_{misfolding}$. Fig. 4 also shows that, once $k_{misfolding}$ allows exponential replication, $k_{melting}$ just sets the exponential growth rate of the replication reaction. These conclusions are robust for a wide range of $k_{kinetic\ trap}$, confirming that the melting and misfolding rates basically control the efficiency of self-replication.

As a general principle, the second role of bond optimization is to increase the probability of formation of transient n_c-contact structures that can fold into the desired cluster. In the octahedron
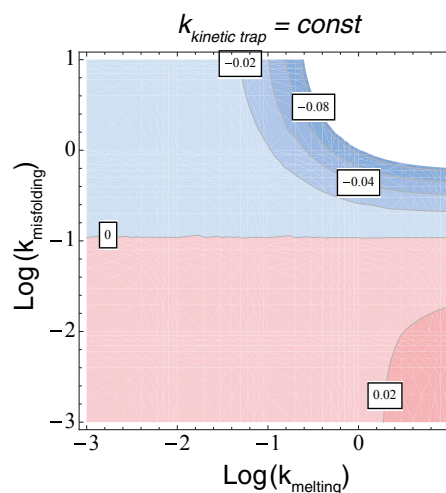

Fig. 4. Contour map of the replication growth rate as a function of melting and misfolding rates. Kinetic trap rate is kept constant. The blue contours correspond to negative growth and pink to positive growth rates.

example, using the value $n_c = 9$, this effect is less prominent. Our bond optimization is naively not expected to suppress the undesired nine-contact transient structure (marked red in Fig. 1*C*), but still the replication rate is much improved due to suppression of the kinetic trap. For a given cluster and choice of n_c, bond optimization can be guided by suppression of kinetic traps and boosting of final folding, although possibly only a balance between the two will give the optimal replication and error rates. It is worth noting that the existence of the trade-off between misfolding (error) rate and melting (replication) rate is well established in protein synthesis and other biosynthetic activities (like chromosome replication and transcription) (20, 21). In our system as well, this balance is intrinsic, reflecting the fact that replication proceeds autonomously.

Following the principles explained above, we created schemes for self-replicating three other clusters: (*i*) two different schemes for the polytetrahedron ($N = 6$) (Fig. 5 *A* and *B*) requiring a dimer catalyst; (*ii*) pentagonal bipyramid ($N = 7$) (Fig. 5*C*) requiring a trimer catalyst; (*iii*) chiral ($N = 7$) cluster (Fig. 5*D*) requiring a dimer catalyst. It is noteworthy that the $N = 7$ chiral cluster can replicate, preserving its chirality when $n_c = n_c^{max} = 14$. If $n_c \le 13$, the replication process creates copies with both chiralities. These examples suggest that the ability of a cluster to self-replicate might not depend so much on its geometry.

The number of different particle types required for realizing any of these schemes depends on the design of actual clusters. Like the octahedron, to ensure that a desired cluster is the only ground state, we need to use a number of different particle types obeying certain interaction rules. For a given cluster, the solution to this problem is not necessarily unique (13). Even without going into details, we can give upper bounds for the number of different particle types, M, needed for self-replicating schemes in Fig. 5: (*i*) the polytetrahedron (schemes a and b) can be designed with at most 5 different particle types, implying the total number of different particle types is $M = 2 \cdot 5 + 2 \cdot 2 = 14$, where we account for the cluster, its catalyst, and their complements; (*ii*) the pentagonal bipyramid (scheme C) can be designed with at most 6 particle types, implying $M = 2 \cdot 6 + 2 \cdot 3 = 18$ because the catalyst is a trimer; (*iii*) the chiral cluster (scheme D) can be designed with at most 7 particle types, implying $M = 2 \cdot 7 + 2 \cdot 2 = 18$.

Next, we discuss possible experimental realizations of our protocol. The replication schemas described here were inspired by colloidal particles coated with DNA that have already been realized and used for self-assembly (22–26). Although our description assumes particles with isotropic interactions, the use of
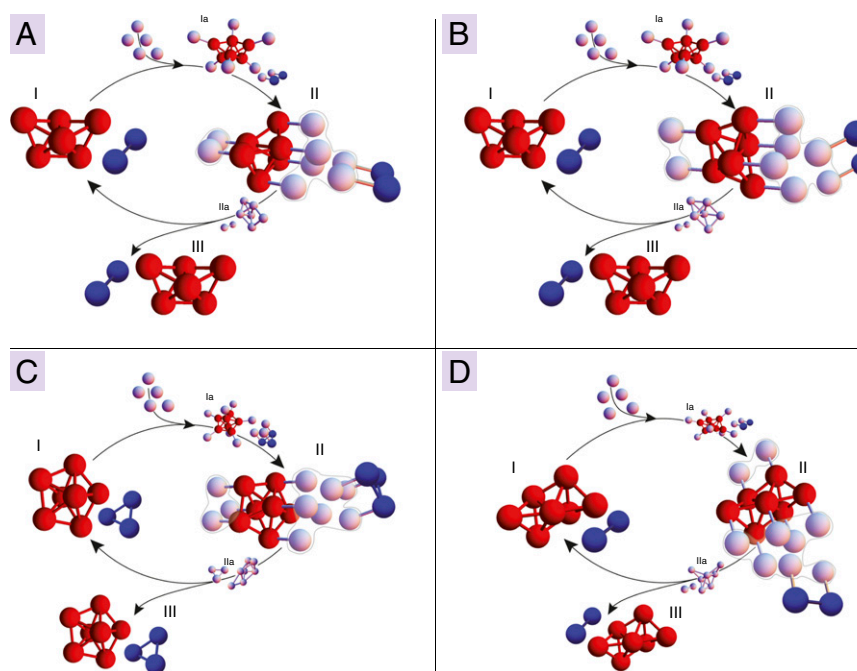
Fig. 5. Self-replication schemes for various clusters. (*A* and *B*) Two different self-sustained reaction schemes for self-replication of a $N = 6$ polytetrahedral cluster (red particles). A minimal catalyst needed for the replication is a dimer (blue particles). (*C*) Self-sustained reaction scheme for self-replication of a $N = 7$ pentagonal bipyramid (red particles). A minimal catalyst needed for the replication is a trimer (blue particles). (*D*) Self-sustained reaction scheme for self-replication of a chiral $N = 7$ cluster (red particles). A minimal catalyst needed for the replication is a dimer (blue particles).

particles with bond directionality is also possible (27–29) and would lower the number of different particles types required to implement our schemes. The essential ingredients could just as well be encoded with other materials, e.g., proteins (10).

The most difficult part of the experimental realization appears to be the melting process, where we require that melting is locally triggered when attached monomers form n_c bonds. In general, as n_c is being reached, each formed bond decreases the energy of the floppy attached cluster. Once attached monomers have enough contacts between themselves, this floppy cluster signals both the seed cluster and the catalyst to release all of their extra bonds, which requires an input of energy (*SI Text*). With present technology for building blocks, it is not straightforward to trigger local melting. This would require the development of methods for achieving colloidal interactions with positive and negative cooperative binding and other allosteric mechanisms. Another, currently accessible, way for exploring our schemes is to modulate the particle interactions with light and temperature cycling; this is currently the standard experimental method for achieving replication with linear structures (9).

To conclude, we emphasize that the vast majority of replication schemes studied so far, such as those based on linear molecules (9), are inspired by DNA and represent "symbolic replication," which is irrespective of size and shape. However, the replication mechanism of other biological objects, such as Golgi apparatus, endoplasmatic reticulum, and micelles (30–33), is firmly tied to their geometrical shape. Our schemas are closer to the latter mechanism of geometry-based replication, which could be a significant advantage in building bulk materials. Finally, we note that, although we have demonstrated the possibility of coding a replication reaction into the interactions between particles in compact clusters, an important open question is whether such schemes can be designed for arbitrarily large compact structures.

Materials and Methods

A detailed description of our simulation together with two simulation movies (Movies S1 and S2) and a movie that demonstrates the replication scheme shown in Fig. 1*A* (Movie S3) is included in *SI Text*.

1. Giver L, Gershenson A, Freskgard P-O, Arnold FH (1998) Directed evolution of a thermostable esterase. *Proc Natl Acad Sci USA* 95(22):12809–12813.
2. Arnold FH (2001) Combinatorial and computational challenges for biocatalyst design. *Nature* 409(6817):253–257.
3. Von Neumann J, Burks AW (1966) *Theory of Self-Reproducing Automata* (Univ of Illinois Press, Urbana, IL).
4. Nobili R, Pesavento U (1994) John von Neumann's Automata Revisited. *Artificial Worlds and Urban Studies.* eds Bessusi E, Cecchini A (DAEST Publication, Convegni 1, Venezia).
5. Sipper M (1998) Fifty years of research on self-replication: An overview. *Artif Life* 4(3): 237–257.
6. Chou H-H, Reggia JA (1998) Problem solving during artificial selection of self-replicating loops. *Physica D* 115:293–312.
7. Penrose LS (1959) Self-reproducing machines. *Sci Am* 200:105–114.
8. Penrose LS (1958) Mechanics of self-reproduction. *Ann Hum Genet* 23(1):59–72.
9. Wang T, et al. (2011) Self-replication of information-bearing nanoscale patterns. *Nature* 478(7368):225–228.
10. King NP, et al. (2012) Computational design of self-assembling protein nanomaterials with atomic level accuracy. *Science* 336(6085):1171–1174.
11. Meng G, Arkus N, Brenner MP, Manoharan VN (2010) The free-energy landscape of clusters of attractive hard spheres. *Science* 327(5965):560–563.
12. Arkus N, Manoharan VN, Brenner MP (2009) Minimal energy clusters of hard spheres with short range attractions. *Phys Rev Lett* 103(11):118303.
13. Hormoz S, Brenner MP (2011) Design principles for self-assembly with short-range interactions. *Proc Natl Acad Sci USA* 108(13):5193–5198.
14. Eigen M, Schuster P (1977) The Hypercyde: A principle of natural self-organization. *Naturwissenschaften* 64:541–565.
15. Eigen M, Schuster P (1978) The hypercycle part B. *Naturwissenschaften* 65:7–41.
16. Eigen M, Schuster P (1978) The hypercycle part C. *Naturwissenschaften* 65:341–369.
17. Müller-Herold U (1983) What is a hypercycle? *J Theor Biol* 102:569–584.

18. Hoogerbrugge PJ, Koelman JMVA (1992) Simulating microscopic hydrodynamic phenomena with dissipative particle dynamics. *Europhys Lett* 19(3):155–160.

19. Groot R, Warren P (1997) Dissipative particle dynamics: Bridging the gap between atomistic and mesoscopic simulation. *J Chem Phys* 107(11):4423–4435.

20. Johansson M, Lovmar M, Ehrenberg M (2008) Rate and accuracy of bacterial protein synthesis revisited. *Curr Opin Microbiol* 11(2):141–147.

21. Murugan A, Huse DA, Leibler S (2012) Speed, dissipation, and error in kinetic proofreading. *Proc Natl Acad Sci USA* 109(30):12034–12039.

22. Mirkin CA, Letsinger RL, Mucic RC, Storhoff JJ (1996) A DNA-based method for rationally assembling nanoparticles into macroscopic materials. *Nature* 382(6592):607–609.

23. Valignat MP, Theodoly O, Crocker JC, Russel WB, Chaikin PM (2005) Reversible self-assembly and directed assembly of DNA-linked micrometer-sized colloids. *Proc Natl Acad Sci USA* 102(12):4225–4229.

24. Biancaniello PL, Kim AJ, Crocker JC (2005) Colloidal interactions and self-assembly using DNA hybridization. *Phys Rev Lett* 94(5):058302.

25. Park SY, et al. (2008) DNA-programmable nanoparticle crystallization. *Nature* 451(7178): 553–556.

26. Macfarlane RJ, et al. (2011) Nanoparticle superlattice engineering with DNA. *Science* 334(6053):204–208.

27. Suzuki K, Hosokawa K, Maeda M (2009) Controlling the number and positions of oligonucleotides on gold nanoparticle surfaces. *J Am Chem Soc* 131(22): 7518–7519.

28. Kim J-W, Kim J-H, Deaton R (2011) DNA-linked nanoparticle building blocks for programmable matter. *Angew Chem Int Ed Engl* 50(39):9185–9190.

29. Wang Y, et al. (2012) Colloids with valence and specific directional bonding. *Nature* 491(7422):51–55.

30. Alberts B, et al. (2002) *Molecular Biology of the Cell* (Garland Science, New York).

31. Munro S (2002) More than one way to replicate the Golgi apparatus. *Nat Cell Biol* 4(10):E223–E224.

32. Bachmann PA, Luisi PL, Lang J (1992) Autocatalytic self-replicating micelles as models for prebiotic structures. *Nature* 357:57–59.

33. Fellermann H, Solé RV (2007) Minimal model of self-replicating nanocells: A physically embodied information-free scenario. *Philos Trans R Soc Lond B Biol Sci* 362(1486): 1803–1811.

PHYSICS